

# Green Synthesis and Antibacterial Evaluation of Silver Nanoparticles using *Senna surattensis* Extracts

Mustafa Jadoua, Munther Abduljaleel Muhammad-Ali, Nassir Abdullah Alyousif \*

Department of Ecology, College of Science, University of Basrah, Basrah, Iraq; kareemmustafa043@gmail.com (M.J.); munther.ali@uobasrah.edu.iq (M.A.M.)

\* Correspondence: nassir.hillo@uobasrah.edu.iq

## Abstract

Green synthesis of silver nanoparticles (AgNPs) using plant extracts is among the simplest, most convenient, economical, and environmentally friendly approaches, as it reduces the use of toxic chemicals. This study aimed to biosynthesize AgNPs using *Senna surattensis* and to evaluate both the plant extracts and the resulting nanoparticles as antibacterial agents. Aqueous extracts were prepared using three methods, and AgNPs were produced by adding silver nitrate to these extracts. Ultraviolet-visible (UV-Vis) spectroscopy, scanning electron microscopy (SEM), X-ray diffraction (XRD), Fourier-transform infrared (FTIR) spectroscopy, and gas chromatography-mass spectrometry (GC-MS) were employed to characterize the nanoparticles. The antibacterial activity of the extracts and AgNPs against various Gram-positive and Gram-negative bacteria isolated from hospital wastewater was assessed at three concentrations: 25, 35, and 50 mg/mL. The largest inhibition zone for the plant extracts alone was 25 mm against *Kocuria rosea* using the Soxhlet acetone extract at 50 mg/mL, whereas the smallest was 12 mm against *Pseudomonas aeruginosa* and *Serratia marcescens* using the cold-soak extract and the Soxhlet aqueous extract at 35 and 25 mg/mL, respectively. Additionally, the cold-soaked extract, the 50 °C hot-soaked extract, and the Soxhlet water extract showed no activity at 25 and 35 mg/mL. For AgNPs derived from *S. surattensis* extracts, the highest inhibition zone was 26 mm against *P. aeruginosa* using AgNPs from the Soxhlet aqueous extract at 50 mg/mL, while the lowest was 14 mm against *Escherichia coli* using AgNPs from the Soxhlet aqueous extract at 35 mg/mL. These findings indicate that AgNPs biosynthesized from *S. surattensis* extracts are promising antibacterial agents and may serve as viable alternatives to conventional antibiotics.

**Keywords:** antibacterial activity; green synthesis; *Senna surattensis*; silver nanoparticles; wastewater

**Type:** Original Article

Received: 17 July 2025; Revised: 27 August 2025; Accepted for publication: 21 September 2025; Published online: 22 September 2025

## 1. Introduction

Water pollution is a major challenge in both developing and industrialized countries. Rapid population growth increases the release of chemicals, microorganisms, and other toxic substances, leading to the deterioration of drinking-water quality [1]. These pollutants enter the environment through multiple pathways, including livestock and agricultural waste, human excreta, pharmaceutical wastewater, and improper disposal practices [2].

Microbial contamination of urban water is a global public-health concern, especially in developing countries. Bacteria are the predominant microbial pathogens in drinking water. The principal sources of waterborne pathogens include livestock feces, sewage, industrial wastewater, and pharmaceuticals [3, 4]. People who consume contaminated water may develop diarrhea, and inadequate water and sanitation services further raise the incidence of diseases such as cholera, schistosomiasis, and helminth infections. Unsafe drinking water can also cause gastrointestinal illness that impairs nutrient absorption and leads to malnutrition, effects that are particularly pronounced in children [5, 6].

Plant-based green synthesis of nanoparticles has gained significant attention as a sustainable, eco-friendly alternative to conventional chemical and physical methods for producing antimicrobial agents [7]. Nanoparticles are solid particles at the atomic or molecular level with sizes <100 nm and often exhibit superior physical properties compared with bulk materials, depending on size and morphology [8]. Owing to their small size and high surface-to-volume ratio, silver nanoparticles may display antimicrobial activity beyond that of ionic silver, and their size and shape can be tuned by the manufacturing process [9]. Compared with other biogenic routes (e.g., microbial synthesis, which requires complex culture maintenance), plant extracts offer a simpler pathway for nanoparticle production. Thus, plant-assisted synthesis can be greener and more sustainable than traditional methods by optimizing energy and resource use according to the nanoparticles' requirements [10].

This approach is also quick, safe, and cost-effective, consuming less energy and yielding non-toxic derivatives. The resulting nanoparticles possess diverse, useful properties for applications across multiple fields [11]. Plant extracts are complex mixtures that

may have antioxidant, antibiotic, antiviral, antibacterial, anticancer, antiparasitic, antifungal, and insecticidal activities [12]. Constituents such as flavonoids, amino acids, proteins, polysaccharides, enzymes, polyphenols, steroids, and reducing sugars facilitate the reduction, formation, and stabilization of nanoparticles [13]. *Senna surattensis* is widespread in tropical and subtropical countries and is used as food and in herbal preparations: roots are used to treat gonorrhea and snakebite, leaves for dysentery, and flowers as a laxative. Crude extracts of *S. surattensis* have demonstrated antimicrobial and antioxidant properties [14]. The present study aimed to perform green synthesis of silver nanoparticles using leaf extracts of *S. surattensis* and to determine the antimicrobial properties of the extracts and biosynthesized nanoparticles against bacteria isolated from local hospital wastewater.

## 2. Materials and Methods

### 2.1 Collection of Plant Samples

*S. surattensis* plants were collected at the University of Basrah, Karma Ali (30.571497, 47.748086) during November–December 2024. The plants were placed in plastic bags, transported to the laboratory, washed with distilled water to remove dust, and air-dried for one week. The dried material was then ground with a ceramic mortar and stored as plant powder in labeled plastic containers.

### 2.2 Preparation of the Leaf Extracts

Leaf extracts were prepared in various ways. Cold soaking involved taking 20 g of the leaf plant powder and placing it in a 500 mL conical flask containing 150 mL of distilled water, leaving it for 24 h. It was then filtered using filter paper, and 25 mL was taken for later use, while the remainder was left to dry [15]. Hot soaking involved taking 20 g of the leaf plant powder and placing it in a 500 mL conical flask containing 150 mL of distilled water. It was then heated on a magnetic stirrer plate at a temperature of 50 °C for 2 h. After that, it was filtered using filter paper, and 25 mL was taken for later use, while the remainder was left to dry [16]. Using the Soxhlet apparatus, aqueous and alcoholic extracts were prepared by taking 20 g of the leaf plant powder, placing it inside a thimble, and using water, alcohol, and acetone sequentially as solvents. Then 25 mL was taken for later use, while the remaining was dried in dishes, ground, and stored in plastic containers [17].

### 2.3 Green Synthesis of Nanoparticles

Silver nanoparticles (AgNPs) were prepared by taking 25 mL of the selected plant extract solution and placing it in a 500 mL glass flask containing 150 mL of deionized distilled water. Then, 0.2 g of silver nitrate was added, and the mixture was heated on a magnetic stirring hot plate at 50 °C with stirring. After that, it was stored for one day in a closed place. Then, it was placed in Petri dishes and left to dry. After that, the particles were ground and stored in plastic containers [18].

### 2.4 Characterization of AgNPs

A variety of physical techniques were used to determine and confirm the nanostructural characteristics of the plant extracts and AgNPs. Gas chromatography–mass spectrometry (GC–MS; Agilent Technologies, USA) was employed to analyze components of the aqueous extract. The optical properties of AgNPs were investigated using an ultraviolet–visible (UV–Vis) spectrophotometer over 200–

700 nm. Fourier-transform infrared (FTIR) spectroscopy (Shimadzu, Japan) was used to analyze the dried extract material and AgNPs. X-ray diffraction (XRD) using the following Debye–Scherrer equation and scanning electron microscopy (SEM) were used to examine the structural properties, particle size, and morphology of the AgNPs [19]:

$$D = \frac{K \lambda}{\beta \cos \theta}$$

where D is the crystallite size, K is the Scherrer constant (typically around 0.9),  $\lambda$  is the wavelength of the X-rays,  $\beta$  is the peak broadening at half maximum intensity (FWHM) in radians, and  $\theta$  is the Bragg angle.

### 2.5 Isolation and Identification of Bacterial Species

#### 2.5.1 Sample Collection

Samples of wastewater were collected from Al-Mawani General Hospital and Al-Fayhaa Hospital in Basrah Governorate during the period from November 1, 2024, to December 12, 2024. The water samples were collected at a depth of 10–15 cm, with 0.5 L taken using a sterile plastic container from several points. They were placed in sterile laboratory plastic containers, transported to the laboratory, and stored in a refrigerator at 4 °C until laboratory analyses were conducted.

#### 2.5.2 Isolation of Bacterial Species

The serial dilution method was used to isolate bacteria from wastewater. First, 1 mL of water was added to 9 mL of sterile distilled water to achieve a  $10^{-1}$  dilution. Then, 1 mL was transferred with a sterile pipette to another tube containing 9 mL of sterile distilled water to obtain a  $10^{-2}$  dilution. This process was repeated sequentially to reach a  $10^{-6}$  dilution. Plates containing nutrient agar were then inoculated under sterile conditions with 0.1 mL of sample, in duplicate for each dilution, and the inoculum was spread over the surface with a sterile glass spreader. The plates were incubated at 37 °C for 24 h, after which the cultured bacteria were examined.

#### 2.5.3 Purification of Bacterial Isolates

Positive bacterial isolates identified in the preliminary examination were purified by transferring portions of colonies to fresh plates containing nutrient agar. The plates were incubated at 37 °C for 24 h. Purity was confirmed by Gram staining and light microscopy. The pure colonies were then preserved on nutrient agar slants and stored in a refrigerator at 4 °C.

#### 2.5.4 Identification of Bacterial Isolates

The pure bacterial isolates were activated on nutrient agar and transported to Al-Fayhaa Hospital in a cooling box for identification using the VITEK 2 system. The VITEK 2 system was used in accordance with the manufacturer's instructions, employing ID Gram-Positive and ID Gram-Negative cards for identification.

### 2.6 Antibacterial Activity of Plant Extracts and AgNPs

The agar well diffusion method was utilized to assess the activity of the extracts and AgNPs at concentrations of 25, 35, and 50 mg/mL. These extracts were dissolved in 1 mL of DMSO and left for at least 3 h to ensure thorough dissolution. The bacterial species isolated from hospital wastewater were activated individually on

Mueller–Hinton agar. A volume of 0.1 mL of each dissolved extract and of the AgNPs was added to the wells of the cultured bacterial plates, which were then incubated at 37 °C for 24 h. The inhibition zones of the plant extracts and AgNPs against bacterial colony growth were determined by measuring the diameter of the inhibition zone for each bacterial isolate [20].

### 3. Results and Discussion

#### 3.1 Characterization of Plant Extracts

GC–MS revealed a range of aromatic and aliphatic compounds. Figure 1 indicates the components of the aqueous extract of *S. surattensis* prepared by the cold-soaking method. High-abundance constituents belonged to phenols, alcohols, carboxylic acids, and heterocyclic compounds, with proportions from 26.74% to 1.25%. These GC–MS findings for *S. surattensis* extracts were consistent with those in a previous study [21].

For the 50 °C hot-soak extract of *S. surattensis*, active chemicals included phenols, alcohols, carboxylic acids, and amines, with concentrations ranging from 38.27% to 0.94% (Figure 2). In the Soxhlet-derived aqueous extract, the major classes comprised phenols, alcohols, organosilicon compounds, and esters, with concentration ratios from 62.54% to 0.88% (Figure 3). In the Soxhlet alcoholic extract, detected actives included phenols, alcohols, and cyclic esters, with concentrations from 10.01% to 2.16% (Figure 4). In the Soxhlet acetone extract, prominent constituents were cholesterol derivatives, alcohols, and phenols, with concentrations ranging from 45.33% to 2.14% (Figure 5).

#### 3.2 AgNPs Synthesis using Plant Extracts and AgNPs Characterization

The fundamental color change from green to dark brown indicated the synthesis of AgNPs using an aqueous extract of *S. surattensis* leaves and silver nitrate at a concentration of 0.2 g. The reduction of silver ions ( $\text{Ag}^+$ ) causes surface plasmon resonance oscillation, which is essential for the formation of silver nanoparticles [22], as shown in Figure 6.

The UV–Vis spectrophotometer is a widely used spectroscopic device to confirm the formation of AgNPs in solution through the phenomenon of surface plasmon resonance of metallic nanoparticles. This optical property is sensitive to the size, shape, concentration, and agglomeration state of the produced nanoparticles. The ultraviolet and visible spectrum confirmed the formation of AgNPs biosynthesized from the *S. surattensis* plant using the cold soaking, hot soaking at 50 °C, and Soxhlet methods, as shown in Figure 7. The AgNPs were observed using the ultraviolet and visible spectrum, with the highest absorption peaks appearing at wavelengths of 440, 410, and 440 nm [23]. The current study is consistent with the study of Hamid et al. [24], who demonstrated the UV–Vis spectrum of AgNPs biosynthesized from the plant *Melia azedarach* at wavelengths ranging from 300 to 900 nm, with an absorption peak at 430 nm indicating the formation of silver nanoparticles.

The basic structures of the AgNPs biosynthesized from the *S. surattensis* plant were identified using three different extraction methods (cold soaking, hot soaking at 50 °C, and Soxhlet) and analyzed using energy-dispersive X-ray spectroscopy (EDX). It was found that the AgNPs contained several compounds. The results showed that the highest percentage of AgNPs was obtained using the Soxhlet extraction method, reaching 64.39% in the plant, as

shown in Table 1 and Figure 8. The present study is consistent with the previous research [25], which reported the biosynthesis of AgNPs from *Senna occidentalis*. The EDX spectra of the AgNPs indicated that the sample consisted of 10.01% silver, with a notable peak at 3 keV, suggesting the reduction of silver ions ( $\text{Ag}^+$ ) to  $\text{Ag}^0$ . Additionally, the EDX spectrum revealed the presence of carbon, sodium, chlorine, and other elements, along with complementary mineral elements.

XRD is considered one of the most important techniques used to determine the composition of biologically synthesized nanoparticles, as it is non-destructive, rapid, and highly capable in material characterization. The XRD pattern for the AgNPs from the cold-soaked *S. surattensis* extract exhibited a peak intensity of 100% (Table 2; Figure 9). Applying the Debye–Scherrer equation yielded an average crystallite size of 25.76% for the biologically synthesized AgNPs. This study is consistent with a previous report [26].

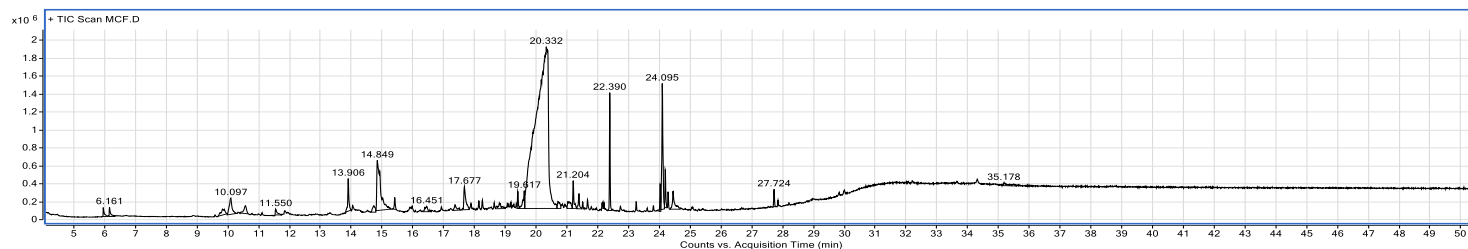
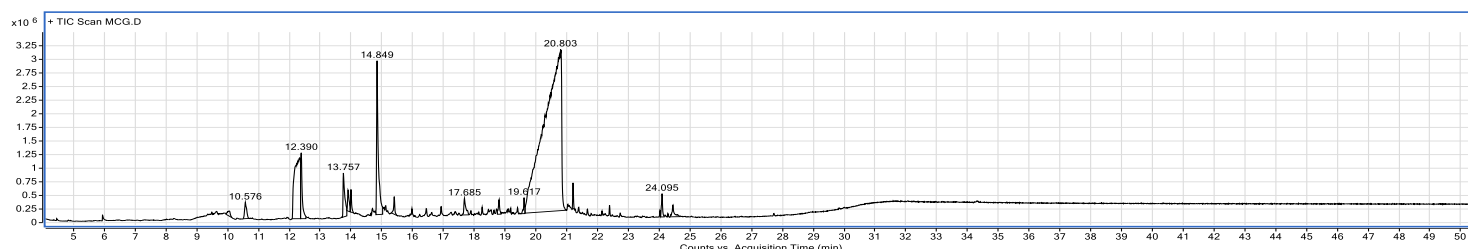
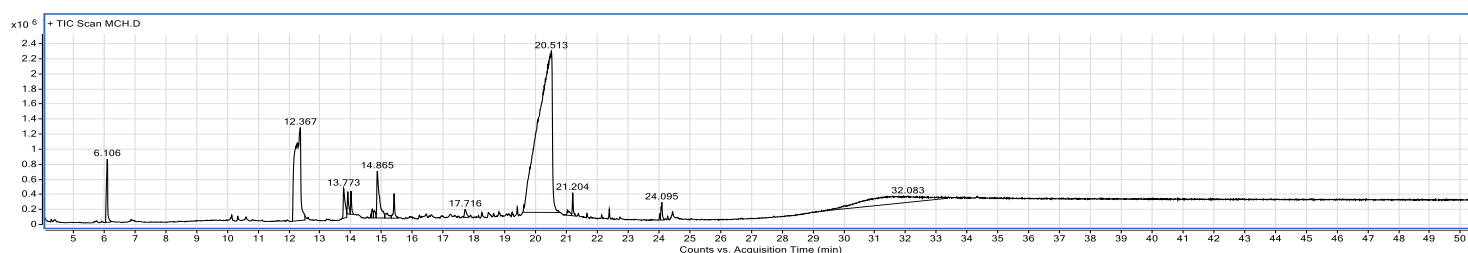
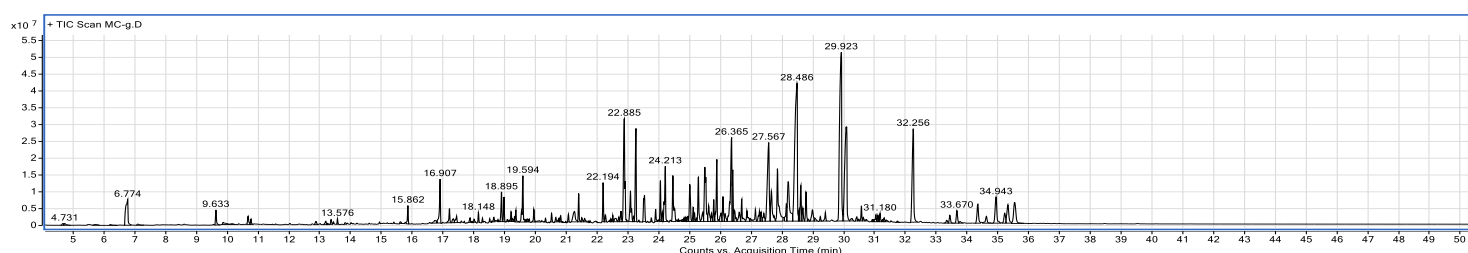
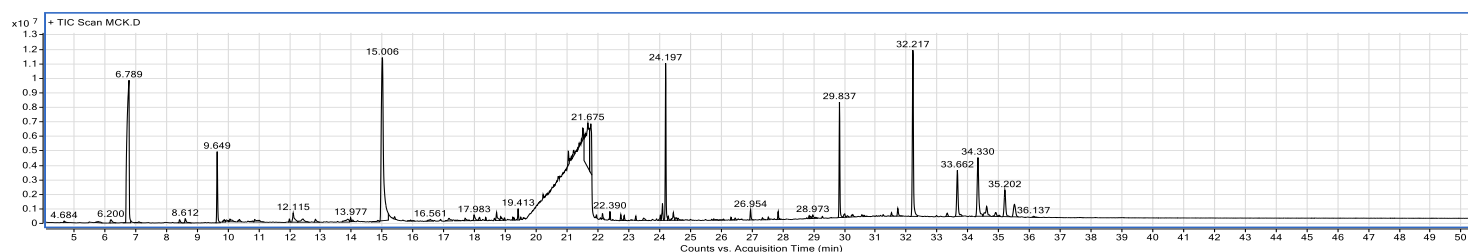
For the 50 °C extract, the XRD profile of the *S. surattensis* AgNPs likewise showed a 100% peak intensity (Table 3; Figure 9). Using the Debye–Scherrer equation, the average crystallite size of the biologically synthesized AgNPs was 22.80%. For AgNPs obtained via Soxhlet extraction of *S. surattensis* using water as the solvent, the XRD spectrum showed a maximum peak of 100% (Table 4; Figure 9). The Debye–Scherrer calculation indicated an average crystallite size of 33.37% for the biologically synthesized AgNPs.

Morphologies and surface sizes of AgNPs synthesized from the *S. surattensis* plant were determined using SEM. Imaging showed that the AgNPs were smooth and spherical, with an average size of 65.15 nm for the cold-soaked extract. For the hot extract at 50 °C, the average size was 32.88 nm, while the Soxhlet extract yielded nanoparticles with an average size of 52.24 nm. The current study is consistent with the study of Samuggam et al. [27], which indicated biosynthesized AgNPs from *Spondias mombin* measuring 17 nm, as shown in Figure 10.

#### 3.3 Antibacterial Activity of Plant Extracts and AgNPs

The current study has isolated several bacterial species from hospital wastewater, originating from patients, hospital workers, and other sources; as a result, most of these bacteria are pathogenic. The activity of the *S. surattensis* plant extract against Gram-negative and Gram-positive bacteria isolated from hospital wastewater was evaluated. The extract was obtained using three methods, including cold soaking, hot soaking, and Soxhlet extraction, with three concentrations of 25, 35, and 50 mg/mL using the diffusion method. The results showed the antibacterial activity of the plant extracts from *S. surattensis* by measuring the diameter of the inhibition zone against the growth of Gram-positive bacteria. The highest inhibition zone was 25 mm against *Kocuria rosea*, resulting from the use of the acetone Soxhlet extract at a concentration of 50 mg/mL, whereas the lowest inhibition diameter was 12 mm when using the aqueous Soxhlet extract at a concentration of 25 mg/mL against *Leuconostoc mesenteroides*. While other extracts of *S. surattensis* did not show effectiveness against bacterial growth, as shown in Table 5.

For Gram-negative bacteria, the activity test of the *S. surattensis* plant extract showed the highest inhibition zone of 21 mm in diameter against *Citrobacter sedlakii* using the acetone Soxhlet extract at a concentration of 50 mg/mL, while the lowest inhibition zone of 12 mm in diameter was recorded against *Pseudomonas*

Figure 1: GC-MS chromatogram of cold-soaked extract of *S. surattensis*.Figure 2: GC-MS chromatogram of hot-soaked extract at 50 C° of *S. surattensis*.Figure 3: GC-MS chromatogram of Soxhlet aqueous extract of *S. surattensis*.Figure 4: GC-MS chromatogram of Soxhlet alcoholic extract of *S. surattensis*.Figure 5: GC-MS chromatogram of Soxhlet acetone extract of *S. surattensis*.

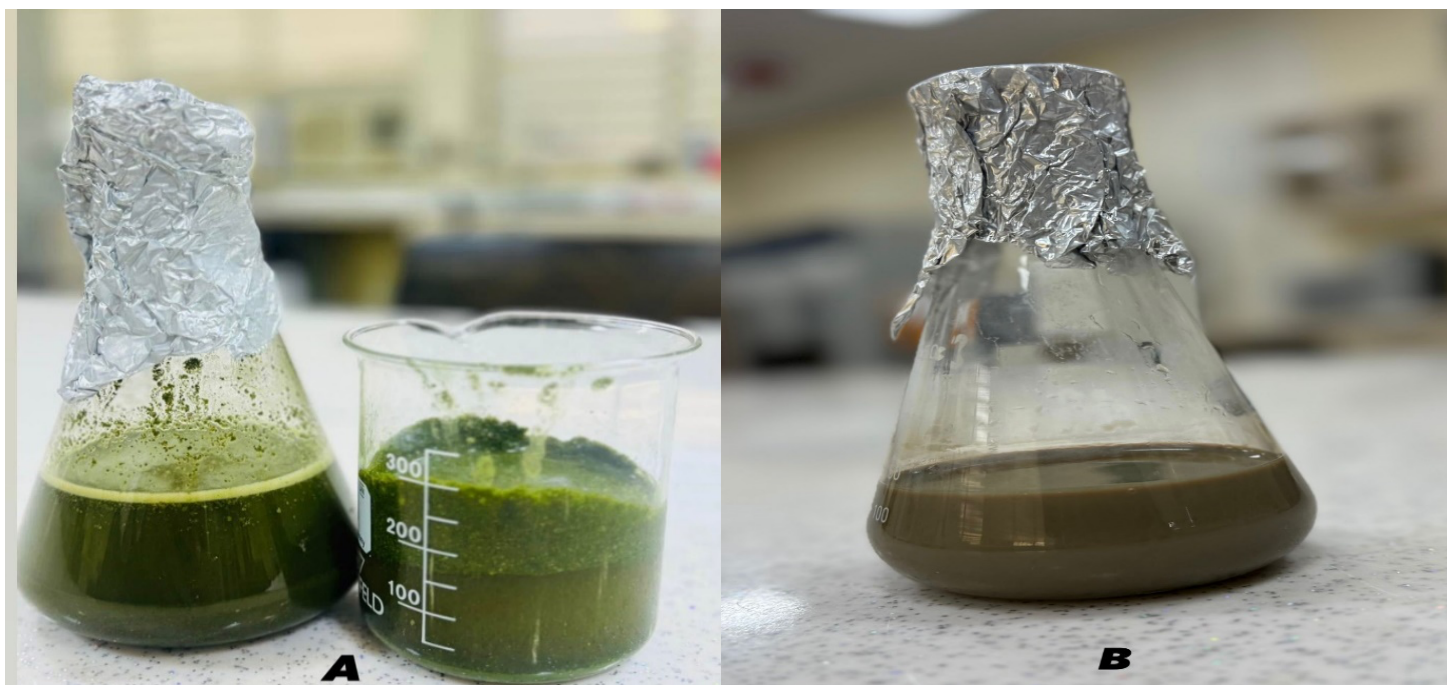


Figure 6: Synthesis of AgNPs. A: Green color of the extract before addition of silver nitrate. B: Brown color of the extract after silver nitrate addition.

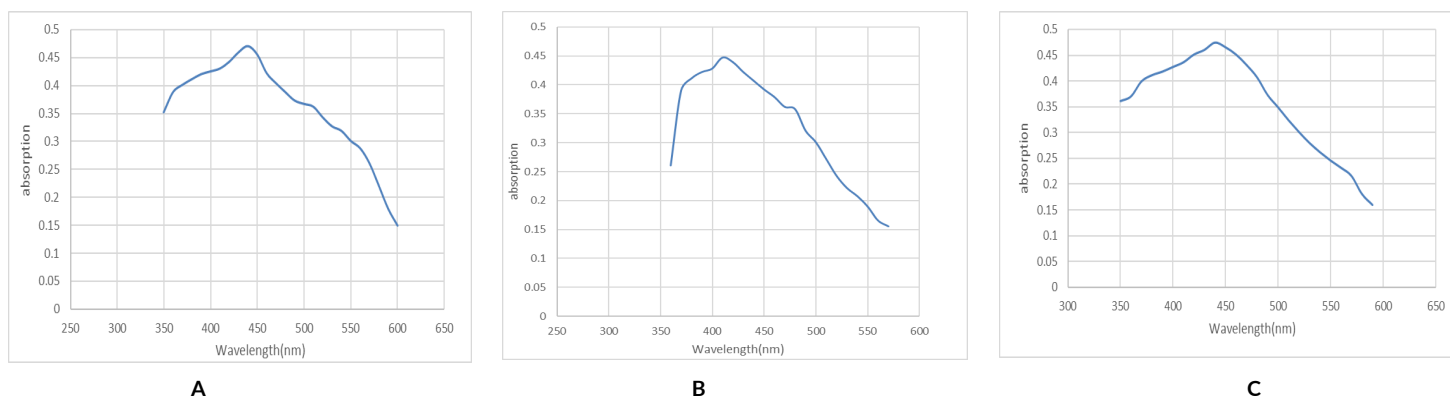


Figure 7: UV-Vis profiles for AgNPs synthesized from *S. surattensis*. A: Cold-soaked. B: Hot-soaked at 50 °C. C: Soxhlet aqueous extraction.

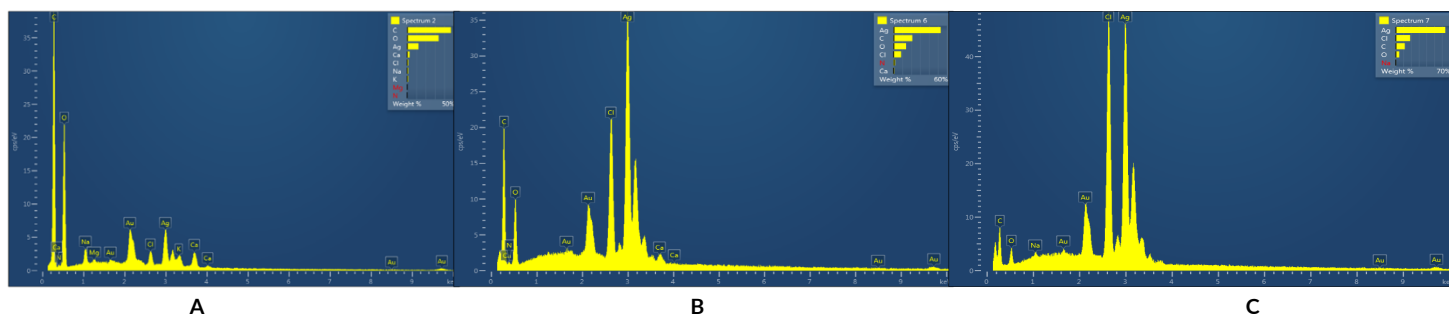


Figure 8: EDX spectra for AgNPs synthesized from *S. surattensis*. A: Cold-soaked. B: Hot-soaked at 50 °C. C: Soxhlet aqueous extraction.

Table 1: Percentage (%) of silver (Ag), carbon (C), and oxygen (O) in AgNPs manufactured by green synthesis.

Type of nanoparticles	% of Ag	% of O	% of C
Cold-soaked	12.17	34.00	47.24
Hot-soaked at 50 °C	53.10	14.24	21.27
Soxhlet aqueous	64.39	4.67	11.86

Table 2: XRD spectrum data for the AgNPs biosynthesized from the cold-soaked extract of *S. surattensis*.

Pos. (°2θ)	Height (cts)	FWHM (°2θ)	d-spacing (Å)	Rel. Int. (%)
27.8387	29.68	0.1968	3.20482	61.78
32.2251	48.04	0.3149	2.77790	100.00
38.1694	21.75	0.3149	2.35786	45.29
44.3539	6.49	0.4723	2.04239	13.51
46.2350	28.69	0.4330	1.96358	59.72
54.8564	8.67	0.3149	1.67363	18.04
57.4735	6.56	0.4723	1.60349	13.66
64.3976	3.59	0.6298	1.44679	7.47
77.1024	5.38	1.1520	1.23601	11.21

Table 3: XRD spectrum data for AgNPs biosynthesized from the hot-soaked extract at 50 °C of *S. surattensis*.

Pos. (°2θ)	Height (cts)	FWHM (°2θ)	d-spacing (Å)	Rel. Int. (%)
27.7609	11.25	0.3149	3.21362	36.58
32.1694	27.74	0.3149	2.78258	90.19
38.0417	30.76	0.3936	2.36548	100.00
44.2179	9.55	0.4723	2.04835	31.04
46.2410	14.94	0.3149	1.96334	48.57
54.9699	2.50	1.2595	1.67045	8.13
64.4812	3.73	0.9446	1.44512	12.14
77.3505	6.10	1.3440	1.23266	19.84

Table 4: XRD spectrum data for AgNPs biosynthesized from the Soxhlet aqueous extract of *S. surattensis*.

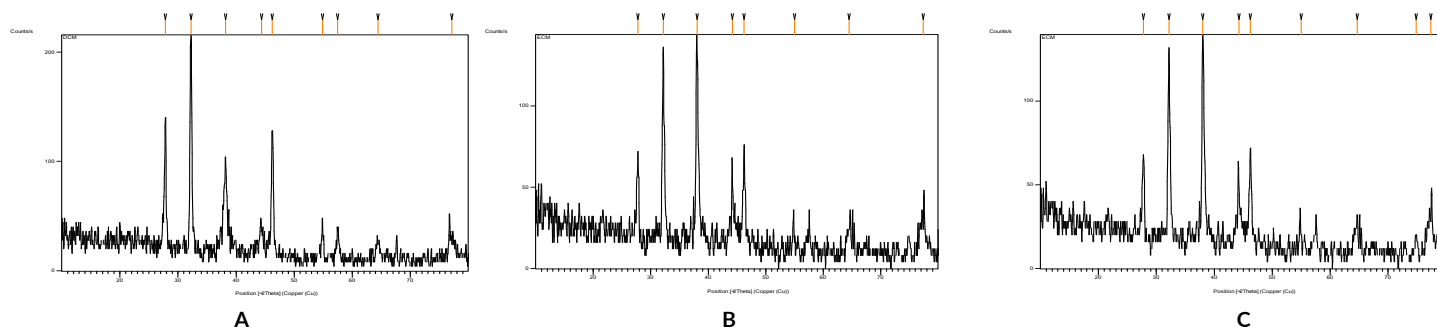
Pos. (°2θ)	Height (cts)	FWHM (°2θ)	d-spacing (Å)	Rel. Int. (%)
27.7703	11.76	0.2755	3.21255	38.21
32.1703	27.04	0.3149	2.78251	87.88
38.0145	30.77	0.2362	2.36710	100.00
44.2290	9.58	0.4723	2.04787	31.13
46.2363	14.41	0.3936	1.96353	46.85
54.9917	2.08	1.2595	1.66984	6.76
64.6565	3.65	0.9446	1.44163	11.87
74.8462	2.68	0.6298	1.26862	8.72
77.3528	6.28	1.3440	1.23263	20.41

*aeruginosa* and *Serratia marcescens* due to the use of the cold-soak extract at a concentration of 35.25 mg/mL, respectively. Additionally, other extracts of the *S. surattensis* plant did not show any activity at certain concentrations, as shown in Table 6 and Figure 11.

The results showed that the highest inhibitory activity against the growth of Gram-positive bacteria was observed for the acetone Soxhlet extract, due to its content of bioactive compounds against bacterial growth, such as cholesterol derivatives, alcohols, and phenols. The effect of this extract is attributed to the sensitivity of Gram-positive bacteria's cell-wall structure to plant extracts; additionally, the absence of an outer membrane enhances permeability, leading to destruction of the bacterial membrane and inhibition of biofilm formation, DNA synthesis, and protein synthesis [28]. The current study is consistent with the study of

Okla et al. [29], who prepared primary extracts of roots, stems, leaves, fruits, and seeds of the *Avicennia marina* plant in ethanol, which were then fractionated into ethanol, ethyl acetate, petroleum ether, chloroform, and water.

In the study of Okla et al. [29], the minimum inhibitory concentration of the extracts against *Bacillus subtilis*, *Escherichia coli*, *P. aeruginosa*, and *Staphylococcus aureus* was also determined. It was observed that the chloroform extract from *A. marina* roots exhibited inhibitory effects against *S. aureus* (MIC =  $1.5 \pm 0.03$  mg/mL) and *E. coli* (MIC =  $1.7 \pm 0.01$  mg/mL). The ethanolic extract of *A. marina* roots showed antibacterial activity against *P. aeruginosa* (MIC =  $10.8 \pm 0.78$  mg/mL), *B. subtilis* (MIC =  $6.1 \pm 0.27$  mg/mL), *S. aureus* (MIC =  $2.3 \pm 0.08$  mg/mL), and *E. coli* (MIC =  $6.3 \pm 0.28$  mg/mL). The ethyl acetate extract of *A. marina* leaves also showed antibacterial activity against *S. aureus* and *E. coli*.

Figure 9: XRD spectra for AgNPs synthesized from *S. surattensis*. A: Cold-soaked. B: Hot-soaked at 50 °C. C: Soxhlet aqueous extraction.



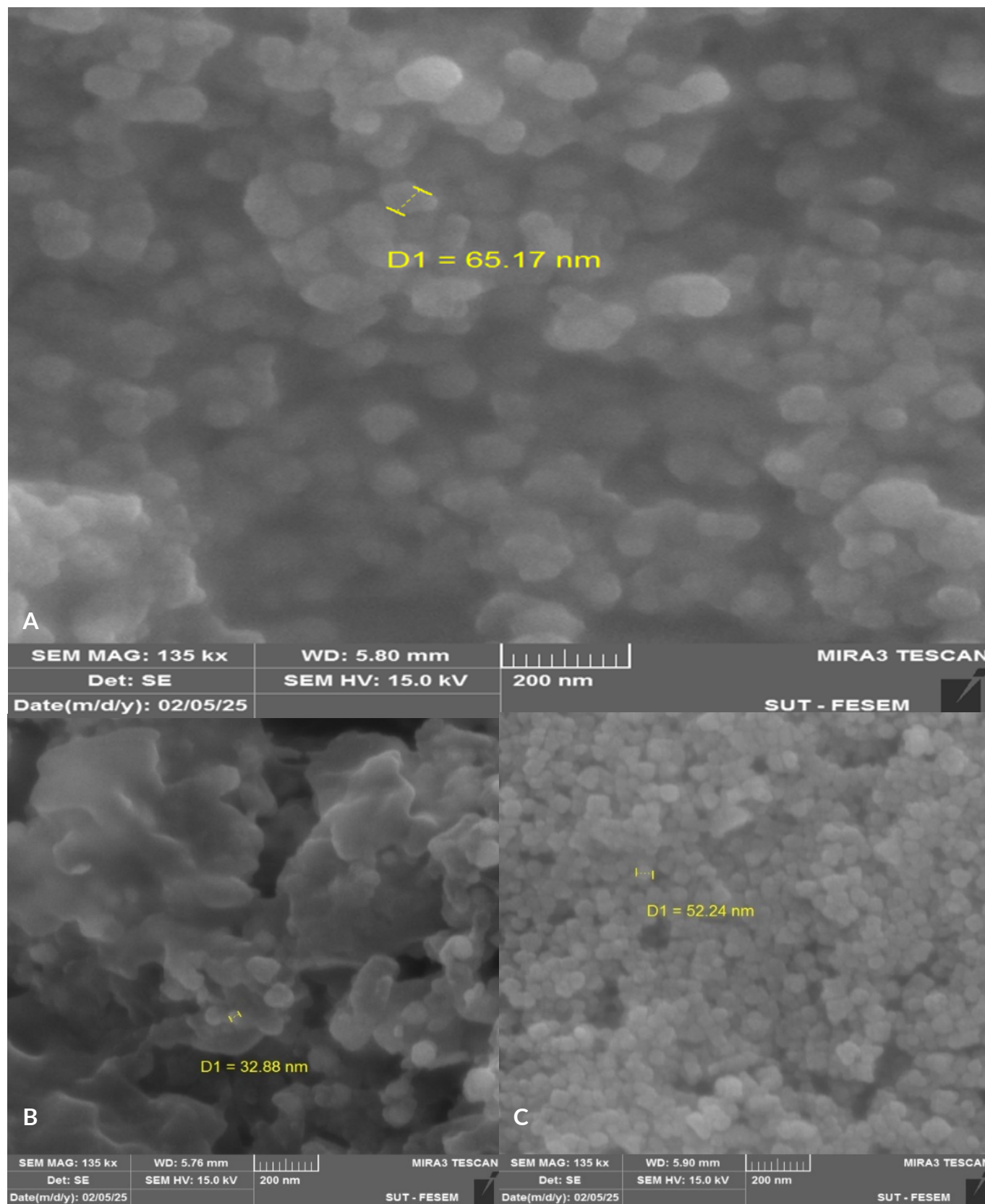


Figure 10: SEM for AgNPs synthesized from *S. surattensis*. A: Cold-soaked. B: Hot-soaked at 50 °C. C: Soxhlet aqueous extraction.

Table 5: Antibacterial activity of *S. surattensis* extracts against Gram-positive bacteria isolated from hospital wastewater.

Extract	Concentration (mg/mL)	<i>L. mesenteroides</i>	<i>K. rosea</i>	<i>S. hominins</i>
Cold-soaked	25	12	0	0
	35	0	0	0
	50	0	18	16
Hot-soaked at 50 °C	25	16	0	0
	35	0	0	0
	50	0	17	17
Soxhlet aqueous	25	14	0	0
	35	0	0	0
	50	0	21	14
Soxhlet alcohol	25	17	14	16
	35	13	15	14
	50	18	20	16
Soxhlet acetone	25	17	15	17
	35	14	15	15
	50	18	25	19

Table 6: Antibacterial activity of *S. surattensis* extract against Gram-negative bacteria isolated from hospital wastewater.

Extract	Concentration (mg/ml)	<i>E. coli</i>	<i>E. cloacae</i>	<i>P. aeruginosa</i>	<i>C. sedlakii</i>	<i>M. morganii</i>	<i>S. marcescens</i>
Cold-soaked	25	16	0	12	0	14	0
	35	0	0	15	0	13	12
	50	13	14	0	17	17	14
Hot-soaked at 50 °C	25	14	0	13	16	18	0
	35	0	0	13	0	14	13
	50	14	17	15	18	19	14
Soxhlet aqueous	25	17	0	14	17	15	0
	35	0	0	14	0	16	15
	50	14	13	13	19	20	18
Soxhlet alcohol	25	17	16	15	17	17	15
	35	15	16	17	16	17	17
	50	16	18	17	20	17	18
Soxhlet acetone	25	18	17	19	16	16	15
	35	17	16	18	17	16	18
	50	18	19	18	21	20	19

Figure 11: Diffusion assay of *S. surattensis* extract showing antibacterial activity against (A) *S. hominis* and (B) *S. marcescens*; halos indicate growth inhibition.



Table 7: Antibacterial activity of AgNPs biosynthesized from *S. surattensis* against Gram-positive bacteria isolated from hospital wastewater.

Type of AgNPs	Concentration (mg/ml)	<i>L. mesenteroides</i>	<i>K. rosea</i>	<i>S. hominins</i>
Cold-soaked	25	18	16	18
	35	17	17	18
	50	20	23	20
Hot-soaked at 50 °C	25	15	14	18
	35	17	17	18
	50	19	21	18
Soxhlet aqueous	25	18	17	20
	35	17	19	17
	50	19	25	19

Table 8: Antibacterial activity of AgNPs biosynthesized from *S. surattensis* against Gram-negative bacteria isolated from hospital wastewater.

Type of AgNPs	Concentration (mg/ml)	<i>E. coli</i>	<i>E. cloacae</i>	<i>P. aeruginosa</i>	<i>C. sedlakii</i>	<i>M. morganii</i>	<i>S. marcescens</i>
Cold-soaked	25	17	15	19	17	18	15
	35	16	17	20	16	17	16
	50	17	17	23	18	17	19
Hot-soaked at 50 °C	25	17	16	20	18	17	16
	35	14	15	21	16	18	15
	50	16	15	24	17	18	20
Soxhlet aqueous	25	19	19	21	19	18	17
	35	15	18	22	17	18	17
	50	21	18	26	19	23	20

Figure 12: Diffusion assay of AgNPs biosynthesized from *S. surattensis* showing antibacterial activity against A: *E. coli*, B: *S. hominins*; halos indicate growth inhibition.

Alemu et al. [30] conducted a study on the antibacterial activity of five selected medicinal plant species, namely *Solanum somalense*, *Verbascum sinaiticum*, *Rumex nervosus*, *Withania somnifera*, and *Calpurnia aurea*. They prepared ethanol and aqueous extracts from plant materials. The results indicated antibacterial efficacy in the ethanolic extracts of *S. somalense*, *W. somnifera*, and *C. aurea* against certain bacterial strains: *S. somalense* against *Streptococcus agalactiae* with a minimum inhibitory concentration of 1.5 mg/mL; *W. somnifera* against *S. aureus* and *E. coli*, with a minimum inhibitory concentration of 2 mg/mL; *C. aurea* against *E. coli* and *Klebsiella pneumoniae*, with a minimum inhibitory concentration of 3 mg/mL and 3.5 mg/mL, respectively.

The results of the activity of the silver nanoparticles biosynthesized from the plant *Senna surattensis* against Gram-positive bacteria showed that the highest inhibition zone was 25 mm in diameter against *Kocuria rosea*, resulting from the use of silver nanoparticles biosynthesized from an aqueous Soxhlet extract at a concentration of 50 mg/mL. Meanwhile, the lowest inhibition zone was 15 mm in diameter against *Leuconostoc mesenteroides*, resulting from the use of silver nanoparticles biosynthesized from hot soaking at 50 °C at a concentration of 25 mg/mL, as shown in Table 7.

Meanwhile, the results showed the activity of the AgNPs biosynthesized from the plant *S. surattensis* against Gram-negative bacteria. The highest inhibition zone reached 26 mm in diameter against *P. aeruginosa*, resulting from the use of AgNPs biosynthesized from the aqueous Soxhlet extract at a concentration of 50 mg/mL. Meanwhile, the lowest inhibition zone was 14 mm in diameter against *E. coli*, resulting from the use of AgNPs biosynthesized from the hot-soaking extract at 50 °C at a concentration of 35 mg/mL, as shown in Table 8 and Figure 12.

This result demonstrated that the best inhibitory effect against the growth of Gram-negative bacteria was achieved using AgNPs prepared from the aqueous extract of Soxhlet, due to its content of biologically active compounds against bacterial species. This can be attributed to the release of metal ions, damage to the cell wall and membrane, penetration into cells, DNA damage, the generation of reactive oxygen species (ROS), lipid oxidation, ATP depletion, and harm to biomolecules [31]. The present study is consistent with the study of Ohiduzzaman et al. [21], who evaluated the antibacterial activities of AgNPs based on green banana pulp extract at different concentrations—200 and 400 µg/disc—against two pathogenic bacteria: *E. coli* (Gram-negative) and *Staphylococcus epidermidis* (Gram-positive). For *E. coli*, AgNPs showed a dose-dependent increase in inhibition zones ( $12.6 \pm 0.42$  mm and  $17.3 \pm 0.14$  mm at 200 µg/disc and 400 µg/disc, respectively), while the standard antibiotic showed an inhibition zone of  $8.4 \pm 0.21$  mm. Similarly, against *S. epidermidis*, the AgNPs showed zones of inhibition of  $12.4 \pm 0.49$  mm and  $13.5 \pm 0.49$  mm at the corresponding concentrations, while the standard antibiotic had a zone of  $15.1 \pm 0.28$  mm.

A study conducted by Yassin et al. [32] focused on the easy green synthesis of AgNPs using an aqueous leaf extract from the plant *Origanum majorana*. The research also examined the biological activity of these nanoparticles against drug-resistant bacteria. The disk diffusion method was employed to assess the antibacterial effectiveness of the AgNPs against three multidrug-resistant hospital bacteria. The results indicated that the antimicrobial

activity of the bioactive AgNPs cells showed that the *Klebsiella pneumoniae* strain was the most susceptible at concentrations of 50 and 100 µg/disc, with inhibition zones of 21.57 and 24.56 mm, respectively. This proves that the aqueous leaf extract of *O. majorana* used in the synthesis of small-sized AgNPs has potential antimicrobial activity against drug-resistant bacterial pathogens.

#### 4. Conclusions

The *S. surattensis* leaf extract and the AgNPs produced from it both showed antibacterial activity against bacterial strains isolated from hospital wastewater. The AgNPs synthesized biologically from the *S. surattensis* plant exhibited higher antibacterial activity than the plant extracts alone against both Gram-positive and Gram-negative bacteria. Accordingly, AgNPs derived from *S. surattensis* are promising antibacterial agents and a viable alternative as antimicrobials. Green-synthesized nanoparticles may be applied in various settings to target pathogenic bacteria, especially in water; however, additional studies are needed to confirm safety and environmental compatibility.

#### Acknowledgement

Deepest gratitude is extended to the Department of Ecology at the College of Science, University of Basrah, Iraq, for providing the essential facilities that made this study possible.

#### Conflict of Interest Statement

The authors declare no conflict of interest.

#### Author Contributions

All authors have contributed equally. They have read and agreed to the published version of the manuscript.

#### References

- [1] Sathish, T.; Ahalya, N.; Thirunavukkarasu, M.; Senthil, T.S.; Hussain, Z.; Siddiqui, M. I.H.; Sadasivuni, K.K. A comprehensive review on the novel approaches using nanomaterials for the remediation of soil and water pollution. *Alex Eng J* **2024**, *86*, 373-385. <https://doi.org/10.1016/j.aej.2023.10.038>
- [2] Salahshoori, I.; Mahdavi, S.; Moradi, Z.; Otadi, M.; Kazemabadi, F.Z.; Nobre, M.A.; Mohammadi, A.H. Advancements in molecular simulation for understanding pharmaceutical pollutant adsorption: A state-of-the-art review. *J Mol Liquids* **2024**, *410*, 125513. <https://doi.org/10.1016/j.molliq.2024.125513>
- [3] Mohammad, A.J.; Alyousif, N.A.; Al-Mosawi, U.A.S.; Al-Hejje, M.M. Assessment of water quality supplies in some areas of Basrah Governorate. *Iraq Eco Env Cons* **2021**, *27*, 408-413. <https://www.envirobiotechjournals.com/EEC/v27i121/EEC-58.pdf>
- [4] Rani, D.; Rana, V.; Rani, A.; Malyan, S. K.; Kumar, A.; Dhaka, R. K.; Rana, A. Microbial contamination in municipal water: Potential sources, analytical methods and remediation strategies. In *Algae based bioelectrochemical systems for carbon sequestration, carbon storage, bioremediation and bioproduct generation*; Mahapatra, D.M.; Singh, L.; Kumar, S.S.; Academic Press: USA, 2024; Volume 3, pp. 125-141.
- [5] Lin, L.; Yang, H.; Xu, X. Effects of water pollution on human health and disease heterogeneity: A review. *Front Envir Sci* **2022**, *10*, 880246. <https://doi.org/10.3389/fenvs.2022.880246>
- [6] Al-Khafaji, A.M.; Al-mansoori, A.F.; Alyousif, N.A. Utilizing bioflocclulants produced by bacteria to remediate oil contaminated water. *Pollution* **2025**, *11*, 440-453. <https://doi.org/10.22059/poll.2024.380806.2507>
- [7] Ratan, A.; Kumar, A.; Singh, S. Green synthesis of silver nanoparticles using leaves of *Lantana camara*: Impact of extract quantity, reaction time on shape, size and antibacterial activity. *J Appl Nat Sci* **2025**, *17*, 479-485. <https://doi.org/10.31018/jans.v17i2.6355>
- [8] Vanlalveni, C.; Lallianrawna, S.; Biswas, A.; Selvaraj, M.; Changmai, B.; Rokhum, S.L. Green synthesis of silver nanoparticles using plant extracts and their antimicrobial activities: A review of recent literature. *RSC Advances* **2021**, *11*, 2804-2837. <https://doi.org/10.1039/D0RA09941D>

- [9] Sajid, M.; Plotka-Wasyłka, J. Nanoparticles: Synthesis, characteristics, and applications in analytical and other sciences. *Microchemical J* **2020**, *154*, 104623. <https://doi.org/10.1016/j.microc.2020.104623>
- [10] Mohammadidargah, M.; Pedram, P.; Cabrera-Barjas, G.; Delattre, C.; Nesic, A.; Santagata, G.; Moeini, A. Biomimetic synthesis of nanoparticles: A comprehensive review on green synthesis of nanoparticles with a focus on Prosopis farcta plant extracts and biomedical applications. *Advances in Colloid and Interface Sci* **2024**, *103277*. <https://doi.org/10.1016/j.cis.2024.103277>
- [11] Nguyen, N.T.T.; Nguyen, L.M.; Nguyen, T.T.T.; Nguyen, T.T.; Nguyen, D.T.C.; Tran, T.V. Formation, antimicrobial activity, and biomedical performance of plant-based nanoparticles: A review. *Envir Chem Let* **2022**, *20*, 2531-2571. <https://doi.org/10.1007/s10311-022-01425-w>
- [12] Armendáriz-Barragán, B.; Zafar, N.; Badri, W.; Galindo-Rodríguez, S.A.; Kabbaj, D.; Fessi, H.; Elaissari, A. Plant extracts: from encapsulation to application. *Exp Opin Drug Deliv* **2016**, *13*, 1165-1175. <https://doi.org/10.1080/17425247.2016.1182487>
- [13] Tesfaye, M.; Gonfa, Y.; Tadesse, G.; Temesgen, T.; Periyasamy, S. Green synthesis of silver nanoparticles using *Vernonia amygdalina* plant extract and its antimicrobial activities. *Heliyon* **2023**, *9*, e17356. <https://doi.org/10.1016/j.heliyon.2023.e17356>
- [14] Bargah, R. K.; Paikra, I.; Tirkey, A.; Singh, S.; Singh, A. Estimation of phytochemical constituents, DPPH free radical scavenging activity and FT-IR analysis of flowers extract of *Senna surattensis* (burm. F.). *Pharma Sci* **2024**, *12*, 73-86. <https://doi.org/10.36673/AJRCPS.2024.v12.i02.A09>
- [15] Sankeshwari, R.M.; Ankola, A.V.; Bhat, K.; Hullatti, K. Soxhlet versus cold maceration: Which method gives better antimicrobial activity to licorice extract against *Streptococcus mutans*? *J Sci Society* **2018**, *45*, 67-71. [https://doi.org/10.4103/jss.JSS\\_27\\_18](https://doi.org/10.4103/jss.JSS_27_18)
- [16] Logeswari, P.; Silambarasan, S.; Abraham, J. Synthesis of silver nanoparticles using plants extract and analysis of their antimicrobial property. *J Saudi Chem Society* **2015**, *19*, 311-317. <https://doi.org/10.1016/j.jscs.2012.04.007>
- [17] Mokaizh, A.A.B.; Nour, A.H.; Alazaiza, M.Y.; Mustafa, S.E.; Omer, M.S.; Nassani, D.E. Extraction and characterization of biological phytoconstituents of *Commiphora gileadensis* leaves using soxhlet method. *Processes* **2024**, *12*, 1567. <https://doi.org/10.3390/pr12081567>
- [18] Abdellatif, A.A.; Alhathloul, S.S.; Aljohani, A.S.; Maswadeh, H.; Abdallah, E.M.; Hamid Musa, K.; El Hamd, M.A. Green synthesis of silver nanoparticles incorporated aromatherapies utilized for their antioxidant and antimicrobial activities against some clinical bacterial isolates. *Bioinorganic Chem Appl* **2022**, *2022*, 2432758. <https://doi.org/10.1155/2022/2432758>
- [19] Said, A.; Abu-Elghait, M.; Atta, H.M.; Salem, S.S. Antibacterial activity of green synthesized silver nanoparticles using *Lawsonia inermis* against common pathogens from urinary tract infection. *Appl Biochem Biotechnol* **2024**, *196*, 85-98. <https://doi.org/10.1007/s12010-023-04482-1>
- [20] Balčiūnaitienė, A.; Štreimikytė, P.; Puzerytė, V.; Viškelis, J.; Štreimikytė-Mockeliūnė, Ž.; Maželienė, Ž.; Viškelis, P. Antimicrobial activities against opportunistic pathogenic bacteria using green synthesized silver nanoparticles in plant and lichen enzyme-assisted extracts. *Plants* **2022**, *11*, 1833. <https://doi.org/10.3390/plants11141833>
- [21] Ohiduzzaman, M.; Khan, M.N.I.; Khan, K.A.; Paul, B. Biosynthesis of silver nanoparticles by banana pulp extract: Characterizations, antibacterial activity, and bioelectricity generation. *Heliyon* **2024**, *10*, e25520. <https://doi.org/10.1016/j.heliyon.2024.e25520>
- [22] Revathi, S.; Sutikno, S.; Hasan, A.F.; Altemimi, A.B.; ALKaisy, Q.H.; Phillips, A.J.; Abdelmaksoud, T.G. Green synthesis and characterization of silver nanoparticles (AgNP) using *Acacia nilotica* plant extract and their anti-bacterial activity. *Food Chem Advances* **2024**, *4*, 100680. <https://doi.org/10.1016/j.focha.2024.100680>
- [23] Widadatalla, H.A.; Yassin, L.F.; Alrasheid, A.A.; Ahmed, S.A.R.; Widadatallah, M.O.; Eltilib, S.H.; Mohamed, A.A. Green synthesis of silver nanoparticles using green tea leaf extract, characterization and evaluation of antimicrobial activity. *Nanoscale Advances* **2022**, *4*, 911-915. <https://doi.org/10.1039/d1na00509j>
- [24] Hamid, L.L.; Ali, A.Y.; Ohmayed, M.M.; Ramizy, A.; Mutter, T.Y. Antimicrobial activity of silver nanoparticles and cold plasma in the treatment of hospital wastewater. *Kuwait J Sci* **2024**, *51*, 100212. <https://doi.org/10.1016/j.kjs.2024.100212>
- [25] Arya, A.; Tyagi, P.K.; Bhatnagar, S.; Bachheti, R.K.; Bachheti, A.; Ghorbanpour, M. Biosynthesis and assessment of antibacterial and antioxidant activities of silver nanoparticles utilizing *Cassia occidentalis* L. seed. *Sci Rep* **2024**, *14*, 7243. <https://doi.org/10.1038/s41598-024-57823-3>
- [26] Singh, R.; Hano, C.; Nath, G.; Sharma, B. Green biosynthesis of silver nanoparticles using leaf extract of *Carissa carandas* L. and their antioxidant and antimicrobial activity against human pathogenic bacteria. *Biomolecules* **2021**, *11*, 299. <https://doi.org/10.3390/biom11020299>
- [27] Samuggam, S.; Chinni, S.V.; Mutusamy, P.; Gopinath, S.C.; Anbu, P.; Venugopal, V.; Enugutti, B. Green synthesis and characterization of silver nanoparticles using *Spondias mombin* extract and their antimicrobial activity against biofilm-producing bacteria. *Molecules* **2021**, *26*, 2681. <https://doi.org/10.3390/molecules26092681>
- [28] Jubair, N.; Rajagopal, M.; Chinnappan, S.; Abdullah, N.B.; Fatima, A. Review on the antibacterial mechanism of plant-derived compounds against multidrug-resistant bacteria (MDR). *Evid Based Complement Alternat Med* **2021**, *2021*, 3663315. <https://doi.org/10.1155/2021/3663315>
- [29] Okla, M.K.; Alatar, A.A.; Al-Amri, S.S.; Soufan, W.H.; Ahmad, A.; Abdel-Maksoud, M.A. Antibacterial and antifungal activity of the extracts of different parts of *Avicennia marina* (Forssk.) Vierh. *Plants* **2021**, *10*, 252. <https://doi.org/10.3390/plants10020252>
- [30] Alemu, M.; Lulekal, E.; Asfaw, Z.; Warkineh, B.; Debella, A.; Abebe, A.; Debebe, E. Antibacterial activity and phytochemical screening of traditional medicinal plants most preferred for treating infectious diseases in Habru District, North Wollo Zone, Amhara Region, Ethiopia. *Plos one* **2024**, *19*, e0300060. <https://doi.org/10.1371/journal.pone.0300060>
- [31] Fanoro, O.T.; Oluwafemi, O.S. Bactericidal antibacterial mechanism of plant synthesized silver, gold and bimetallic nanoparticles. *Pharmaceutics* **2020**, *12*, 1044. <https://doi.org/10.3390/pharmaceutics12111044>
- [32] Yassin, M.T.; Mostafa, A.A.F.; Al-Askar, A.A.; Al-Otibi, F.O. Facile green synthesis of silver nanoparticles using aqueous leaf extract of *Origanum majorana* with potential bioactivity against multidrug resistant bacterial strains. *Crystals* **2022**, *12*, 603. <https://doi.org/10.3390/cryst12050603>

**Publisher's Note:** IMCC stays neutral with regard to jurisdictional claims in published maps and institutional affiliations.



Copyright of this article belongs to the journal and the Iligan Medical Center College. This is an open-access article distributed under the terms and conditions of the Creative Commons Attribution (CC BY) license (<http://creativecommons.org/licenses/by/4.0/>).